Anisotropic frequency response of spin-torque oscillators with applied field polarity and direction

Matthew R. Pufall, William H. Rippard, Stephen E. Russek, and Eric. R. Evarts

NIST, Electromagnetics Division, 325 Broadway, Boulder, Colorado 80305, USA

We have measured spin-torque-driven oscillations of $Ni_{80}Fe_{20}$ free-layer nanocontacts as a function of field direction. For a given field axis angle ($10°$ from the surface normal) and magnitude, simply changing the field polarity can significantly alter the device output. The critical current I_c, the frequency of oscillation f, the amplitude, and the f vs current $f(I)$ all change with field polarity and change if the applied field axis is rotated about the surface normal. Spin-torque ferromagnetic resonance measurements show that the linear resonant frequency f and the slope of $f(I)$ at currents much less than I_c also vary by tens of MHz and tens of MHz/mA, respectively, with field polarity. These results are consistent with the idea that the mode excited by spin torque interacts strongly with a different subregion of the magnetization in the vicinity of the contact for each field direction, resulting in potential variations in the anisotropy field, Oersted field, and spin-torque magnitude as a function of field direction.

I. INTRODUCTION

Spin-torque oscillators based on patterned electrical contacts made to continuous spin-valve multilayers exhibit spontaneous oscillations at a critical dc current I_c at a frequency f that is tunable with field and current.[1–3] These oscillations can be broadly understood as a consequence of the spin torque compensating the damping torque, causing the magnetization to precess around the net effective field, i.e., with a macrospin-type model. In such a model, increasing the magnetization precessional angle with increasing current changes the demagnetizing field and results in red or blue frequency shifts with current, depending on the system geometry.[4–7] Although macrospin simulations can capture many of the characteristics of nanocontact-based spin-transfer oscillators (STOs), in general, the details of their behavior are not well understood. For example, the details of the functional form of f vs I for a particular STO, the observed jumps in frequency,[2,3,8] the precise frequency of oscillation, and the presence of multiple frequencies of oscillation, all lack a model or simulations to describe them.[9–12] Furthermore, device-to-device variations for nominally identical devices are large enough[8,13] to complicate potential applications requiring large arrays of oscillators with precise frequency relationships.

In addition, for a given device, variations in device output simply from changing field polarity (for a fixed field axis) have been previously described by several groups but have not yet been reported in a methodical way.[14] These variations are also not readily explainable by a macrospin model with a net effective field set only by the applied field, the saturation magnetization M_s (or $M_{effective}$) of the free layer, and a uniaxial anisotropy. In this paper, we present systematic measurements of the linear and nonlinear precessional responses of a nanocontact spin-torque oscillator as a function of field direction but for fixed field magnitude and field axis angle measured relative to an axis parallel to the surface normal. The magnitude of the variation in the small-angle precession frequency with field polarity [as measured via spin-torque ferromagnetic resonance (ST-FMR)] is consistent with that expected from inhomogeneities in the anisotropy as measured by ferromagnetic resonance (FMR) on macroscopic samples.

The frequency of the large-angle nonlinear response (that is, the dc-driven oscillation) varies with field direction as well but shows frequency differences larger than those expected from anisotropy variations alone. Finally, other characteristics of the resonance (e.g., amplitude and linewidth) also vary with field polarity and direction for both the ST-FMR and the dc-driven oscillations. As we show below, these data are consistent with the idea that the *position* of the resonance under the contact moves in response to the net effective field (which is itself set by variations in the local field due to anisotropy,[15] Oersted field variations, and the applied field direction) as has been observed in some simulations of STOs.[16] This picture of STO dynamics is similar to that used to interpret the variation in oscillation frequencies of vortex cores in confined structures in which the core responded to the local anisotropy[17] but, in this case, with the spin-transfer-induced resonance as the local probe.

This paper is organized in the following way. In the Method section, we present the experimental means by which we characterize the spectral response of the oscillators via both dc-driven spectra and spin-torque FMR. In Sec. A of the Results section, we present data from dc-driven spectra as a function of field direction and, in Sec. B, results from spin-torque FMR. Finally, in the Discussion section, we present various potential mechanisms that may explain the observed variations with field direction. We stress that the data do not unambiguously determine which mechanisms are responsible for the observed variations. We discuss the success that these mechanisms have in describing the data because they are physically reasonable and because they help clarify the experimental constraints and the orders of magnitude of the device variations with field direction. The primary goal of this paper is to present a clear set of data that is, in our experience, *generally representative* of the variations observed in such devices, a set of data that can then be used for comparison to more refined models, and theories of large-angle magnetization dynamics induced by spin-transfer torques at such length scales.

II. METHOD

To quantify variations in device response, nanocontact devices were measured in the following manner. The field
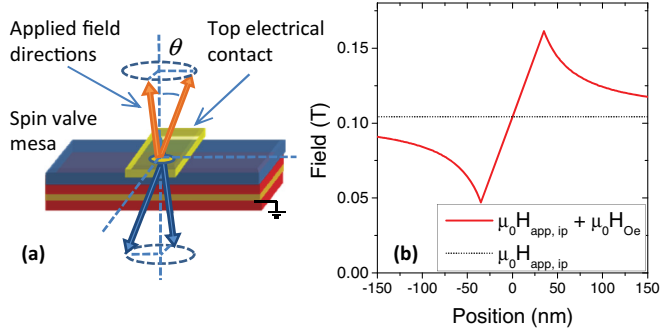
FIG. 1. (Color online) (a) Measurement schematic showing the four applied field directions used in this paper. Sample: 15-nm Cu/10-nm CoFe/4-nm Cu/5-nm $Ni_{80}Fe_{20}$; (b) calculated net in-plane field vs position for 60 nm along an axis perpendicular to the in-plane component of the applied field. Because the Oersted field has a fixed sign, the position of the field minimum switches from one side of the contact to the other with applied field sign. Field angle $\theta_H = 10°$, $|\mu_0 H| = 0.6$ T.

axis was fixed at a given angle (10° from an axis parallel to the nominal surface normal), the accuracy of which is known with an approximate error of 0.5° in our setup, and with a precision of ≈0.1° from sample to sample [see Fig. 1(a)]. The field was set to a saturation value of 0.8 T (defined as positive), then was reduced in magnitude to the measurement field (typically ≈0.6 T for the data presented here), and the dc-driven spin-torque excitation and spin-torque FMR spectra were measured. The uncertainty of the applied field was estimated to be 0.5 mT (5 Oe) for all applied fields. The process was then repeated with the opposite sign of field. The saturation field served to reorient both the free and the fixed layers of the pseudo-spin-valve structures measured here. The sample was then rotated by 90° ± 1° about the surface normal, and the measurements for both signs of field were repeated. The angles of the in-plane projections of the applied fields were measured relative to the top electrical contact of the device [see Fig. 1(a) and schematics in subsequent figures] and are called "parallel" and "perpendicular" to this electrical lead in this paper. With this geometry, a component $H_{app} \sin(10°) = H_{app} \times 0.174$ lies in the film plane and changes direction with field sign and azimuth of the field axis, adding to and subtracting from the circumferential Oersted field due to the dc current through the contact [Fig. 1(b)]. Variations in the order of the uncertainty of the polar field angle can significantly change the ferromagnetic frequency for this field geometry[18,19] so data are quantitatively compared only for a fixed field axis.

For a given sample orientation, this procedure results in two pairs of frequency vs current measurements (one ST-FMR and one dc driven) for which the only change is the sign of the applied field so that their characteristics can be quantitatively compared in a meaningful way. For the dc-driven spectra, the onset current I_c, the frequency f vs current I, and the measured powers can be compared for the two field signs, whereas, for spin-torque FMR spectra, the resonance frequencies vs current for $I < I_c$ can be compared. For both types of spectra, the frequency difference $\Delta f(I) = f_{H^-}(I) - f_{H^+}(I)$ vs I was determined as a quantification of the frequency shifts with field direction.

III. RESULTS

A. Dc-driven spectra

Measurements were made on ≈60-nm diameter contacts made to $Cu_{15}/CoFe_{10}/Cu_4/NiFe_5$ [thicknesses in nanometers (nm)] pseudo-spin-valve structures. The details of the device fabrication can be found in Ref. 2. Data are shown for one nanocontact device. The details of the response are particular to this device, but the observed variations with field direction are, in our experience, typical of similar NiFe/Cu/CoFe pseudo-spin-valve devices measured over several wafers. Figure 2 shows the spectra generated vs dc current as a function of field direction and sign for $|\mu_0 H| \approx 0.620$ T. One can immediately note several qualitative features. First, the critical current I_c varies with field polarity for a given applied field axis and varies when this axis is rotated by 90°, ranging from 8.75 to 10.75 mA for this sample, with an estimated uncertainty on I_c of 0.25 mA.[20] Second, f_{onset} also varies, ranging from 9.335 to 9.780 GHz over the four field directions. Although precise determination of the onset frequency and critical current is difficult due to the small oscillation amplitude at the onset, the range of onset frequencies is, nonetheless, larger than expected from the uncertainty in the applied field magnitude. Variations in field magnitude change the net effective field H_{eff} both through the applied field and through the demagnetizing field by reorientation of **M** and result in a 15–30-MHz frequency variation as estimated from standard thin-film FMR calculations. Finally, the powers and frequencies vs current emitted from the device vary with field direction and polarity. We quantify these variations, which can be determined with greater precision than the onset values, below.
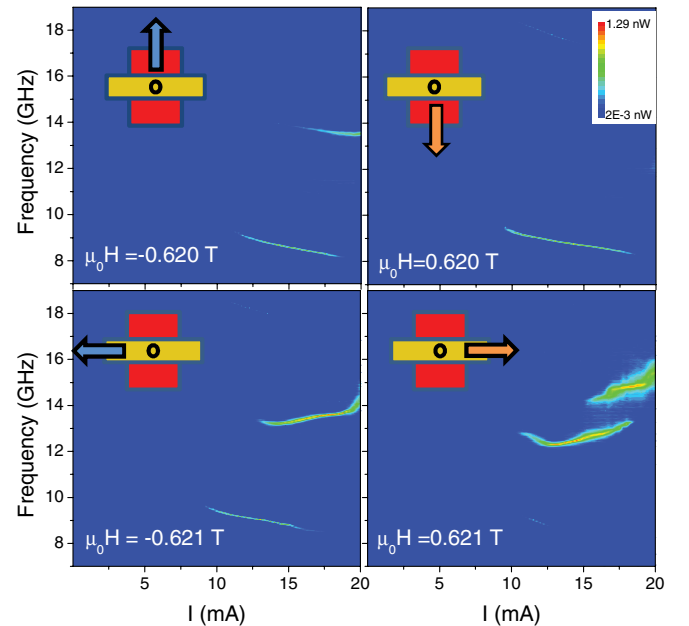

FIG. 2. (Color online) Contour plots of dc-driven spectral output vs field direction and current. Power is a logarithmic scale. Schematics show the direction of the in-plane component of the applied field relative to the top electrical contact; the color of the arrows denotes the sign of out-of-plane field component (light arrow = out of plane).
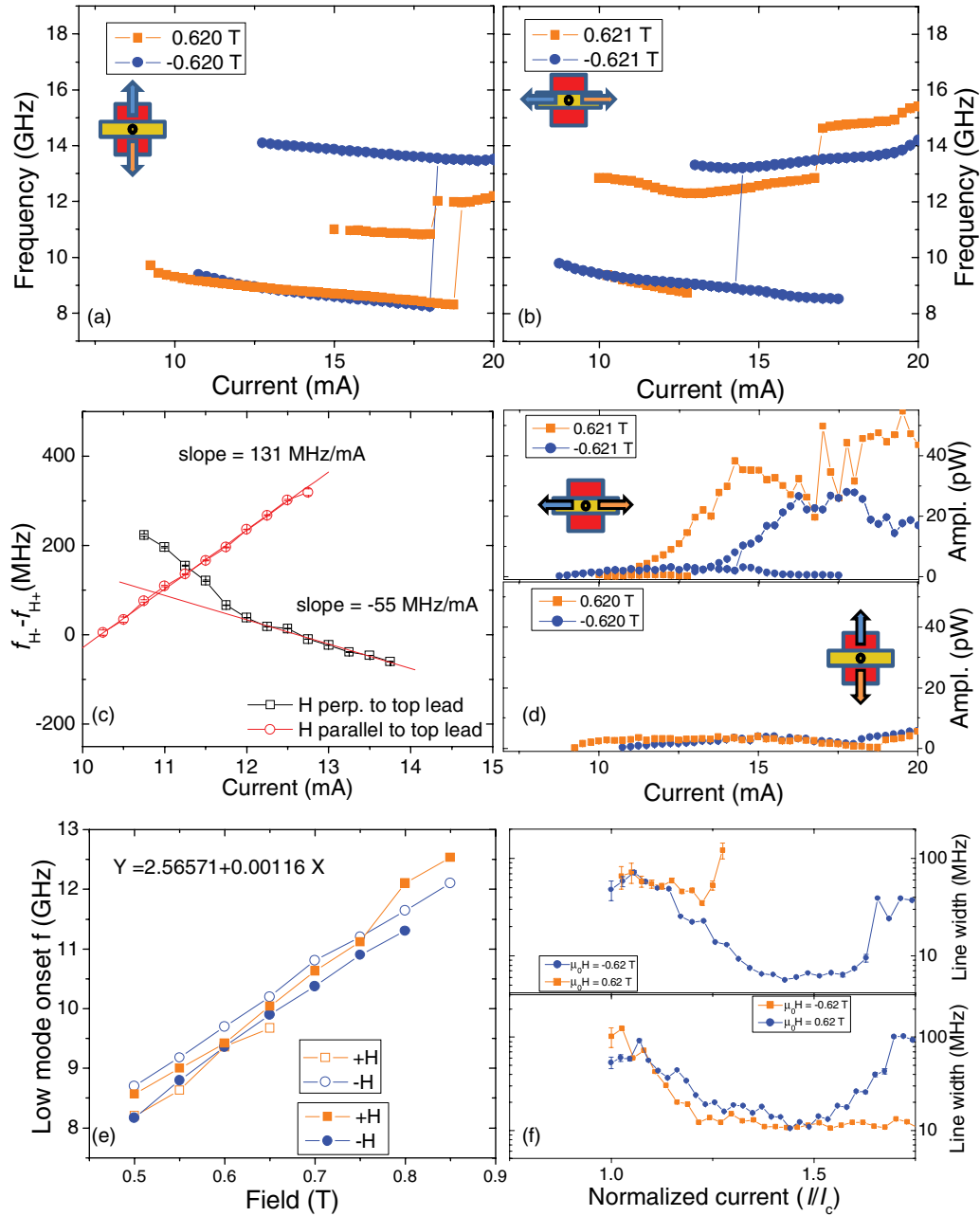
FIG. 3. (Color online) (a) and (b) Fits of major peaks in dc-driven oscillation spectra shown in Fig. 2. (c) Calculated $\Delta f(I) = f_{H^-}(I) - f_{H^+}(I)$. (d) Amplitudes of major peaks vs field axis and current, showing variation with field direction. The lower panel is for data fit in (a), and the upper panel is for data in (b). (e) Onset frequency vs field for four field directions. Closed symbols are for fields oriented as in (a), and open symbols are for fields oriented as in (b). (f) Fitted linewidths vs current normalized by the threshold current I_c.

Center frequencies determined from Lorentzian fits to the major peaks in the spectra for the four field directions are plotted in Figs. 3(a) and 3(b) as functions of current. These plots show that, although the frequencies for the two field signs along a given axis can overlap, in general, the variation in f with I is different for each. Two distinct output frequencies (here, called "modes") are seen from this particular device over a range of currents, a behavior often observed in such devices.[13] The lower-frequency mode may be an in-plane (redshifting with current) mode, whereas, the higher-frequency mode may be an out-of-plane (blueshifting with current) mode

as both have been observed for NiFe-CoFe nanocontacts at these fields and angles.[21] Consistent with this identification, at larger out-of-plane applied fields (≈ 0.9 T, not shown), the lower redshifting mode largely disappears. Upon field reversal, neither mode overlaps over a significant current range for a given field. Indeed, $f(+H)$ and $f(-H)$ of the higher mode are separated by at least 0.5 GHz for the measured spectra. Confining our analysis to the lower-frequency mode just above the onset current (a regime for which models are more likely to be applicable[18]), Fig. 3(c) plots the frequency difference $\Delta f(I) = f_{H^-} - f_{H^+}$ for the two field axes as functions of

current. $\Delta f(I)$ varies in a roughly linear fashion with different slopes for the two field axes. For this device, the slopes of $\Delta f(I)$ have opposite signs, although this is not always the case: In other devices, the slopes of $\Delta f(I)$ can have the same sign. The variation in frequency with field direction is represented in a different way in Fig. 3(e), which plots the frequency at the onset of the low-frequency mode vs applied field magnitude for the four different field directions. Here, variations with field direction are evident, and these data serve to show that the response at 0.6 T is typical for this device.

Other characteristics of the dc-driven oscillations are presented in Figs. 3(d) and 3(f). The fitted output powers for the two field axes are presented in Fig. 3(e) and show significant differences (roughly a factor of 5) in the power between the two axes and smaller differences in the power as a function of field sign along a given axis. In Fig. 3(f), we show the linewidth vs current for the lowest-frequency mode with the current normalized to the estimated critical current I_c for oscillations for that particular field direction (see above). One can note that, at the onset, the linewidths for a given axis are quite similar and decrease with the current in a similar fashion as the current increases just above threshold, before eventually deviating from each other.

B. Spin-torque FMR spectra

The oscillations excited by a dc current in spin-torque oscillators are the result of a nonlinear process.[6,22] In contrast, ST-FMR can measure the *linear* resonant response of the system for dc bias currents well below the critical current for dc oscillations. In ST-FMR, a small ac current is injected into the device, producing an ac spin-transfer torque at the contact. By measuring the rectification voltage generated by the product of the spin-torque-driven ac resistance and the ac current as a function of frequency, one can determine the linear resonance modes of the system. These spectra are shown in Fig. 4. For a given field sign, the device shows a single major feature in the spectrum over the range of frequencies measured (6–16 GHz), consisting of either a single peak or two overlapping peaks. The size of the peak increases as a function of dc current through the contact, reflecting an increase in the fluctuation amplitude with the reduction of the effective damping by the spin torque. We note here that the frequency at which this peak occurs is consistent with that expected from thin-film FMR calculations, given the uncertainties in field angle and $M_{\text{effective}}$.

The position of the ST-FMR peak redshifts with dc-current bias through the contact [Fig. 4(e)], and the rate of this redshift is a function of field direction and sign. This directional dependence is quantified in Fig. 4(f) by plotting $\Delta f(I) = f_{H^-}(I) - f_{H^+}(I)$ for both applied field axes. The function $\Delta f(I)$ is nonzero and approximately linear for both field axes, showing that the resonance responds differently to the combination of Oersted fields and increasing spin torque produced by increasing the current through the contact for the two different field axes. The magnitude and sign of the slope and intercept of $\Delta f(I)$ vary somewhat from contact to contact; for the NiFe/CoFe spin valves studied here, $|\Delta f_{\text{intercept}}| < 100$ MHz and $|\Delta f_{\text{slope}}| < \approx 25$ MHz/mA.

IV. DISCUSSION

A magnetic moment precesses around the net effective field present at its location. In a nanocontact, this field is set by the applied field, the anisotropy fields, the demagnetizing field, the exchange fields, the Oersted field due to the current, and possibly, the spin-torque effective fields from the current. The changes in precession frequency presented above show that the local magnetic environment of the excitation (either dc or ac driven) varies as a function of field direction. In the simple cases of an isotropic film or a film with a uniaxial anisotropy and with the excited mode centered under the nanocontact, $f(+H)$ should equal $f(-H)$ for a given field axis for all currents, which is clearly not the case here. In the following, we discuss some potential mechanisms for the observed variations.

Looking first at the ST-FMR results, Fig. 4(e) shows that the resonance frequencies for a given field axis are similar for low dc currents but redshift at different rates with I. This difference is quantified as $\Delta f(I)$ in Fig. 4(f). Although the signal-to-noise ratios of the spectra are insufficient to reliably fit $f(I)$ for $I < 2$ mA, for 2 mA $< I <$ 7 mA, $\Delta f(I)$ is roughly linear with a nonzero intercept $\Delta f(0)$, suggesting that, along a given applied field axis, the net fields at the resonance point for $+H$ and $-H$ are different. For the NiFe/CoFe spin-valve nanocontacts we have measured, $\Delta f(0)$ was generally nonzero with variations on the order of ± 100 MHz. This corresponds to an effective field variation of $\approx \pm 3.5$ mT (35 Oe) and is consistent with the inhomogeneous linewidth broadening measured in film-level field-swept FMR measurements made on similar spin-valve stacks. From those, we find that a $Cu_{15}/NiFe_5/Cu_3/Ta_3$ stack typically has an inhomogeneous broadening of 0.5–1.0 mT, whereas, the NiFe layer in a full Cu/CoFe/Cu/NiFe spin-valve stack has an inhomogeneous contribution to the linewidth of 4.5–7.5 mT. If this variation in $\Delta f(0)$ is due to anisotropy variations at the resonance position, this implies either that the anisotropy at the contact changes with field sign (through an unknown mechanism) or that the anisotropy is a function of position (such as through roughness or Néel coupling), and the resonant subregion of the magnetization under the contact moves with field polarity and direction.

The above analysis ascribing $\Delta f(0)$ to anisotropy variations relied on the functional forms of $f(I)$ [and, thus, $\Delta f(I)$], which was determined by fits to spectra for $I > 2$ mA, remaining the same for lower currents so that the extrapolation to $I = 0$ was valid. We now discuss other possible mechanisms in addition to anisotropy variations: variations in spin torque and variations in the Oersted field due to the current. For a given current, if precession for one sign of field is driven to a larger cone angle through a more efficient spin-torque process, then the demagnetizing field will be different causing a larger frequency shift at a given current and, hence, a nonzero $\Delta f(I)$. This alternative mechanism still requires some type of anisotropic response such that the device response is a function of applied field sign, for example, by introducing small differences in free- and fixed-layer magnetization angles. If we view the amplitude of the ST-FMR resonance as a measure of the precession angle, it does vary [see Figs. 4(a)–4(d) with field direction in a manner consistent with the idea that the cone angle of the precession varies with field direction,
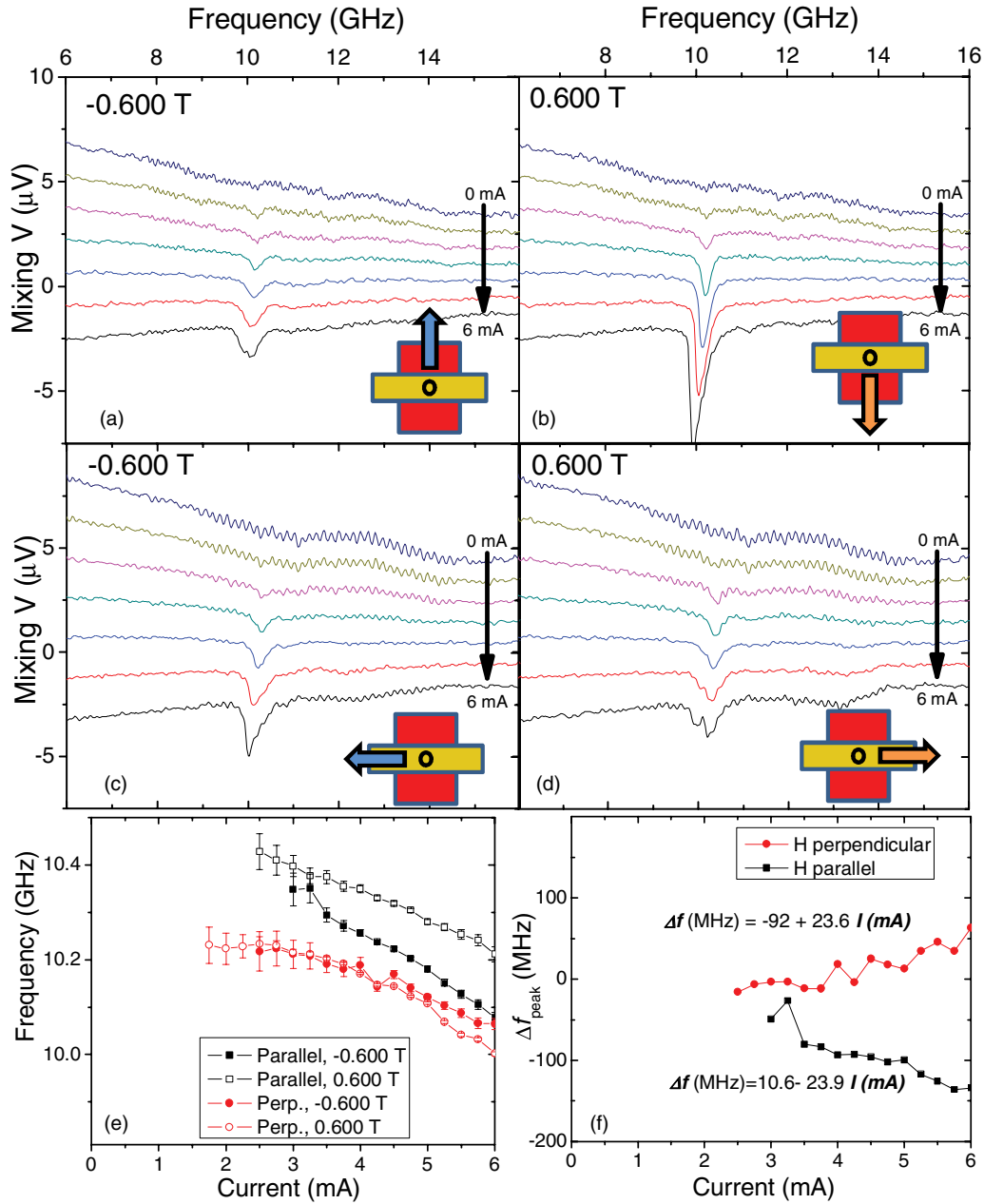
FIG. 4. (Color online) (a)–(d) Spin-torque FMR spectra; (e) spectra vs field direction $f_H(I)$ vs I for four field directions, showing variation with current; (f) $\Delta f(I) = f_{H-}(I) - f_{H+}(I)$ from fits to ST-FMR spectra.

but the ST-FMR response in these metallic nanocontacts at low bias is too small to permit quantitative determinations of the amplitude. Possibly supporting this hypothesis are the similarities of the dc-current-driven linewidths' variations with normalized current shown in Fig. 3(f). Normalizing by the threshold current may account for small variations in spin-torque efficiency.[18]

Another potential mechanism for the increase in magnitude of $\Delta f(I)$ with I as in Fig. 4(f) may be due to variations in the Oersted field—or the effect of the Oersted field—at the excitation location for the different field signs. We find that the slope of $\Delta f(I)$ varies in magnitude and sign from contact to contact with a typical magnitude of ≈ 25 MHz/mA for the contacts studied here. The Oersted field can be appreciable

relative to other fields in the system: For a circular nanocontact of 60-nm diameter, the field at the edge of the contact is ≈ 6 mT/mA.[16] For comparison, the in-plane component of the applied field is ≈ 100 mT for the results presented here. However, the vector sum of the Oersted field over a resonant mode centered under a symmetric contact is zero, so in the simplest approximation, one would expect no variation in the frequency with dc current. More complicated models of the mode's spatial variation are needed to explain a frequency shift for a symmetric configuration.[10,12]

Alternatively, if the resonance is *not* centered on the contact, then the net field seen by the contact varies with the current. With the field applied at 10° to the film normal, the Oersted field adds to the applied field on one side of the contact and

subtracts on the other [see Fig. 1(b)] so that the net field and field angle change as a function of position across the contact. Similarly, if the contact is asymmetric, the Oersted field, as a function of current, is different for different points around the contact. One potential mechanism describing the movement of the resonance position with the field was suggested by Hoefer *et al.* [16] in their micromagnetic simulations in which they showed that, in the case of a single-layer film, the resonance position would occur at the *net field minimum*, over a reasonable range of parameters. In the present case, this minimum is a function of the local anisotropy and the Oersted field as well as the applied field.

The above discussion indicates that the variations in the linear frequency response of the system (i.e., the ST-FMR response) may have several potential explanations with similar orders of magnitude. Their details of the mechanisms are different (variations in anisotropy, spin-torque efficiency, and Oersted field), but all rely on the fact that the excitation is a measure of the local field, and the local field at the excitation varies with applied field direction. These variations in the local field may result in a net field difference for the two signs of field, a change in relative angle between free and fixed layers, or a different current-induced Oersted field response (or a combination of these processes).

In contrast, the variations in the nonlinear response (i.e., the dc-driven resonances) are less readily explained but, nonetheless, show that the net effective field at the resonance varies significantly with field direction and may indicate that the location of the resonant mode under the contact may change with field direction. As seen in Fig. 3(c), just above the critical current for free oscillations, $\Delta f(I)$ was small and increased in magnitude with increasing current as was also the case in ST-FMR. However, at higher current biases, $\Delta f(I)$ can be 1 to 2 GHz for a given value of current. In addition, the curves $f_{H+}(I)$ and $f_{H-}(I)$ are not simply shifted in the current relative to each other as would result from a shift in the critical current I_c but, instead, have somewhat different functional forms. Finally, several peaks are visible in the spectra, the relative powers [Figs. 2 and 3(e)] and positions [Figs. 3(a) and 3(b)] of which vary with field sign and axis.

These high-frequency variations at higher current biases were greater than those expected from the variations in the *static* magnitudes of the local fields, the orders of magnitudes of which were determined from the ST-FMR measurements above. This could imply that the modes excited by dc current respond nonlinearly to these variations in local field or that the effective spin torque due to the current varies significantly as a function of field direction. In addition, coupling of the NiFe layer to the CoFe layer via Néel coupling, which should also be a function of position, may play a role in these spectral variations at larger precession amplitudes. The variation's power observed in Fig. 3(c) may be due to the fact that the nanocontact samples the magnetization dynamics

via giant magnetoresistance (GMR) and, therefore, measures the net magnetic fluctuations only where current flows. If the oscillatory mode moves significantly off center with the field sign, then a smaller net oscillation amplitude may be measured. Also, if the angles of free and fixed layers change significantly with field sign or axis, this changes the sensitivity of the GMR response. Spin-torque efficiency may be similarly affected.

It is worth discussing what measurements might be performed to discern between the various mechanisms presented here. Imaging of the resonant mode with nanometer-scale accuracy would clearly reveal much about the movement of the resonance relative to the contact, but doing so in a working nanocontact device remains a significant measurement challenge.[23] Better understanding of film morphology, both globally (crystallinity and roughness) and locally at the contact (high-resolution TEM) to relate variations in structure to device behavior is also important. Finally, fabrication of devices with strong shape (contact) or film-level anisotropies may show the effect of a clear symmetry/anisotropy axis, rather than the smaller random variations probed here.

V. CONCLUSION

We have shown that, for a given field magnitude and angle to the film plane, the linear and nonlinear frequencies and amplitude responses of spin-torque nanocontacts vary with field direction. By translating the variations in the linear (ST-FMR) response to an effective field variation, we showed that the frequency variations are consistent with measurements of film-level inhomogeneous broadening measurements and consistent with possible variations in net spin-torque efficiency and sensitivity to Oersted fields produced by the current. The variations in the linear resonance frequency with dc current show that the net effective field, including Oersted fields, experienced by the resonance changes with field sign. The frequency variations from nonlinear dc-driven oscillations are larger than those for the linear response, possibly resulting from a nonlinear response of the system to the effective field or a variation in effective spin torque as a function of field direction. These results imply that spin-torque-driven excitations are sensitive to the local magnetic environment on scales less than the nanocontact size in a manner similar to that observed for vortex oscillations in Ref. 17, potentially providing a method of magnetic characterization of unpatterned magnetic films on length scales of tens of nanometers. From the point of view of potential applications, the frequency variations in these oscillators are large enough that their microscopic origins must be understood and must be controlled for systems requiring large arrays of highly similar oscillators. This may require a deeper understanding of film growth, interlayer coupling, fabrication variations, and spin transport on length scales of tens of nanometers.

[1] J. Slonczewski, J. Magn. Magn. Mater. **195**, 261 (1999).

[2] W. H. Rippard, M. R. Pufall, S. Kaka, S. E. Russek, and T. J. Silva, Phys. Rev. Lett. **92**, 027201(2004).

[3] F. B. Mancoff, N. D. Rizzo, B. N. Engel, and S. Tehrani, Appl. Phys. Lett. **88**, 112507 (2006).

[4] G. Bertotti, C. Serpico, I. D. Mayergoyz, A. Magni, M. d'Aquino, and R. Bonin, Phys. Rev. Lett. **94**, 127206 (2005).

[5] S. E. Russek, S. Kaka, W. H. Rippard, M. R. Pufall, and T. J. Silva, Phys. Rev. B **71**, 104425 (2005).

[6] J. Slonczewski, J. Magn. Magn. Mater. **159**, L1 (1996).

[7] S. Bonetti, V. Tiberkevich, G. Consolo, G. Finocchio, P. Muduli, F. Mancoff, A. Slavin, and J. Åkerman, Phys. Rev. Lett. **105**, 217204 (2010).

[8] S. Kaka, M. R. Pufall, W. H. Rippard, T. J. Silva, S. E. Russek, and J. A. Katine, Nature (London) **437**, 389 (2005).

[9] J.-V. Kim, V. Tiberkevich, and A. N. Slavin, Phys. Rev. Lett. **100**, 017207 (2008).

[10] M. d'Aquino, C. Serpico, R. Bonin, G. Bertotti, and I. D. Mayergoyz, Phys. Rev. B **82**, 064415 (2010).

[11] A. Slavin and P. Kabos, IEEE Trans. Magn. **41**, 1264 (2005).

[12] G. Consolo, L. Lopez-Diaz, L. Torres, and B. Azzerboni, Phys. Rev. B **75**, 214428 (2007).

[13] M. R. Pufall, W. H. Rippard, S. E. Russek, S. Kaka, and J. A. Katine, Phys. Rev. Lett. **97**, 087206 (2006).

[14] S. Tamaru and D. S. Ricketts, IEEE Magn. Lett. **3**, 3000504 (2012).

[15] I. Lee, Y. Obukhov, G. Xiang, A. Hauser, F. Yang, P. Banerjee, D. V. Pelekhov, and P. C. Hammel, Nature (London) **466**, 845 (2010).

[16] M. A. Hoefer, T. J. Silva, and M. D. Stiles, Phys. Rev. B **77**, 144401 (2008).

[17] R. L. Compton and P. A. Crowell, Phys. Rev. Lett. **97**, 137202 (2006).

[18] A. Slavin and V. Tiberkevich, IEEE Trans. Magn. **45**, 1875 (2009).

[19] R. D. McMichael, M. D. Stiles, P. J. Chen, and W. F. Egelhoff, J. Appl. Phys. **83**, 7037 (1998).

[20] Determination of I_c from a plot of 1/power vs I (as in Ref. 18) does not decrease the spread in I_c.

[21] S. Bonetti, V. Tiberkevich, G. Consolo, G. Finocchio, P. Muduli, F. Mancoff, A. Slavin, and J. Åkerman, Phys. Rev. Lett. **105**, 217204 (2010).

[22] A. Slavin and V. Tiberkevich, Phys. Rev. Lett. **95**, 237201 (2005).

[23] Y. Acremann, J. P. Strachan, V. Chembrolu, S. D. Andrews, T. Tyliszczak, J. A. Katine, M. J. Carey, B. M. Clemens, H. C. Siegmann, and J. Stöhr, Phys. Rev. Lett. **96**, 217202 (2006).